Research Article

Journal of Environmental Nanotechnology

Influence of Fe_2O_3 Nanoparticle-infused Waste Cooking Oil Biodiesel on the Emission, Performance, and Combustion Aspects towards a Cleaner Environment

J. Allen Jeffrey[1], S. Govindaraj[1], R. Mahesh[2], A. Bhaskar[3], K. Arunkumar[4], R. Edwin Joseph[5], V. Hariram[6*], V. Punitharaj[1] and S. Sarathipriyan[1]

[1]Department of Mechanical Engineering, Loyola Institute of Technology, Chembarambakkam, TN, India
[2]Department of Mechanical Engineering, Aarupadai Veedu Institute of Technology, Vinayaka Mission Research Foundation (DU), Paiyanur, TN, India
[3]Department of Mechanical Engineering, SRM Institute of Science and Technology, Ramapuram, Chennai, TN, India
[4]Department of Automobile Engineering, MLR Institute of Technology, Hyderabad, TG, India
[5]Department of Automobile Engineering, Rajalakshmi Engineering College, Chennai, TN, India
[6]Department of Mechanical Engineering, Hindustan Institute of Technology and Science, Padur, Chennai, TN, India
Received: 23.07.2025 Accepted: 16.09.2025 Published: 30.09.2025
*connect2hariram@gmail.com

ABSTRACT

In the present experimental investigation, Waste cooking oil (WCO) biodiesel was prepared by employing a single-stage transesterification technique using 2.1 grams of NaOH and 65 ml of methanol at a molar ratio of 1:8, at 60 °C for a 75-minute reaction duration, yielding 11.75 liters of WCO biodiesel. Fe_2O_3 nanofluid was prepared using the ultrasonication technique at 60 Hz and 600 rpm for 45 minutes, using deionized ethanol and Sorbitan monooleate solution. The physicochemical properties, including kinematic viscosity, density, calorific value, flash point and fire point, ash content, and cetane index, were found to be within ASTM limits. SEM and stability analyses on Fe_2O_3-suspended diesel-WCO biodiesel blend were also conducted. The test fuel blends of D70WCOB30 and D70WCOB30 with 50 ppm, 100 ppm, and 150 ppm of Fe_2O_3 nanoparticles were prepared separately and tested in a CI engine. The performance test clearly showed that D70WCOB30 Fe_2O_3 NP100 (80% of diesel and 20% of WCOB with Fe_2O_3 nanoparticle doping at 100 ppm) fuel blend produced superior Brake Thermal Efficiency (BTE) and lower Brake Specific Fuel Consumption (BSFC) due to higher calorific value. D70WCOB30 Fe_2O_3 NP100 emitted lower amounts of Unburned Hydrocarbon (UBHC) and CO, whereas the NO_x emissions were notably higher. Lower smoke emissions were seen in a diesel-biodiesel blend with a 50-ppm nanoparticle concentration. The combustion characteristics, including in-cylinder pressure and heat release rate, were positively influenced by the addition of nanoparticles. Overall, the D70WCOB30 Fe_2O_3 NP100 fuel can be used in an unmodified CI engine as a sustainable alternative.

Keywords: Waste cooking biodiesel; Ferric oxide nanoparticles; Nanofluid; Combustion; Emission.

1. INTRODUCTION

The continuous escalation of the human population and the pronounced industrial revolution have greatly increased the use of natural fossil fuels, including gasoline and diesel. As a result, fossil fuels are rapidly depleting due to the continued demand in the energy sector to sustain life on Earth. There is an immediate need to identify a sustainable energy source to address the challenges of the growing energy demand. On the other hand, petro-diesel-fueled transport and the industrial sector release significant amounts of carbon dioxide into the atmosphere, which strongly contribute to global warming. Renewable energy sources such as biodiesel, biohydrogen, and bioethanol are considered more reliable alternatives to petro-diesel, as they help reduce environmental degradation. Vegetable-based biodiesel is one such alternative that can be derived from numerous feedstocks. Its eco-friendliness and better combustion efficacy make it more suitable and feasible to bridge the gap caused by depleting fossil fuels. Vegetable-based biodiesels are non-toxic, biodegradable, renewable, and emit fewer gaseous substances with comparatively higher cetane numbers, better lubricity, higher flash points, and improved combustion efficacy.

Generally, vegetable-based biodiesel possesses triglycerides, which are transesterified into mono-alkyl fatty acid chains through the transesterification process with a base and a catalyst. Vegetable oils are classified as edible oils, which include soybean, groundnut, sunflower, and sesame seeds, and non-edible oils, which

include oil from jatropha, neem, karanja, and mahua. To avoid competition between edible feedstocks, human consumption, and food-based competition, careful consideration was given in selecting the biodiesel feedstock. Waste Cooking Oil (WCO) is one such source of biodiesel feedstock, which may be an appropriate choice as it does not compete with human consumption and is also an effective disposal method. It is estimated that the United Nations alone produces around 3.5 billion gallons of waste cooking oil every year, and its disposal is a critical problem and poses health hazards. Value addition with WCO gained attention from the global research community due to its disposal issue, abundance, availability, and lower cost with minimal environmental degradation.

Gad *et al*. (2022) employed the transesterification process with KOH and methanol to derive biodiesel from waste cooking oil. They have blended 20% of WCO biodiesel with diesel along with 100 ppm of TiO_2, Al_2O_3, and CNT separately to evaluate the engine behaviour when fueled. It was noticed that a nanoparticle blended diesel-biodiesel blend slightly reduced CO, HC, and smoke emission greatly, with a noticeable increase in NO_x emission and peak cylinder pressure. Sonachalam *et al*. (2024) experimented with blends of WCO and diesel with varying proportions of multi-walled CNT (MWCNT) and ethanol in a CI engine to assess the emission, performance, and combustion characteristics employing DOE techniques. It was found that MWCNT at 30 ppm reduced the average fuel consumption greatly with a significant escalation in Brake Thermal Efficiency (BTE). The emissions, including NO_x, CO, and HC, were also reduced considerably due to the 20% ethanol addition. Gad *et al.* (2022) investigated the efficacy of Al_2O_3 nanoparticles in a diesel engine fueled with blends of *Millettia ferruginea* biodiesel and diesel. The suitability of the fuel blend was confirmed by evaluating its physicochemical properties, such as kinematic viscosity, density, flash, fire, cloud, and pour point. BTE was reduced gradually with the increase in the concentration of biodiesel in diesel. Adding Al_2O_3 up to 100 ppm elevated the BTE and reduced the Brake Specific Fuel Consumption (BSFC) considerably, with further diminishing EGT up to 16.6%. HC and CO emission was reduced by 28.52% and 31.23% respectively, with a sharp escalation in NO_x emissions.

Sathish (2024) prepared a hybrid blend of *Azadirachta indica* oil and waste cooking oil biodiesel with diesel and used in a CI engine along with varying proportions of carbon nanotubes as an oxygenate additive. The experiments were conducted by varying the engine load at constant speed. He found that BSFC and BTE escalated significantly with the addition of CNT. Doping the fuel blend with 50 ppm of CNT resulted in optimistic performance with reduced engine emissions. Mubarak *et al.* (2025) mainly analyzed the emission formation in the CI engine when fueled with WCO (20%) and diesel (80%) with varying concentrations of Cerium oxide (CeO2) between 25 ppm and 100 ppm. The CeO_2 nanoparticle was characterized by employing XRD, SEM, and XPS techniques. Additive-activated biodiesel-diesel blend significantly reduced UBHC, CO, and NO_x emissions by 23.46%, 18.27% and 6.57% respectively. A combination of cerium oxide, aluminum oxide, and titanium oxide as oxygenates with Jatropha biodiesel–diesel blends significantly reduced the formation of NO_x, HC, and CO gases. It was also seen that notable improvements in the engine's combustion efficacy were achieved by supplying surplus oxygen during the progressive combustion phase.

A few studies reported the effectiveness of oxygenates, such as Diethyl ether, Diethyl malonate, ethanol, and n-pentanol, on the combustion, performance, and emission of CI engines. Alehegn *et al.* (2025) and Akram *et al.* (2019) demonstrated the usefulness of ethanol addition to Jatropha biodiesel–diesel blend. The outcome showcased an increase in BSFC by 4.32% with considerable emission reduction. Similar parametric studies were conducted by Hoseini *et al*. (2020) on an HCCI engine. Low compression combustion emitted a reduced amount of UBHC and CO with escalated NO_x levels. Muthusamy *et al.* (2018) prepared an emulsion fuel with Jatropha biodiesel fuel blend and infused CNT, which reduced HC and CO emission levels by up to 4.82% and 7.94% respectively. Similarly, Prabu *et al.* (2020) attempted a cleaner combustion process by infusing CNT with a diesel-biodiesel blend in a CI engine. He noticed that the thermal efficiency was considerably increased with a noticeable reduction in exhaust emissions.

It can be noticed that only a few studies have reported the effect of Fe_2O_3 nanoparticles on the diesel-biodiesel blends with insights from the combustion, emission, and performance aspects. The present investigation deals with preparing the Waste cooking biodiesel using a single-stage transesterification process. Fe_2O_3 nanofluid preparation and its characterization were carried out. The Fe_2O_3-doped WCOB fuels were tested, along with straight diesel and WCOB. The effect of the test fuels on the emission, combustion, and performance aspects of an unmodified CI engine was evaluated in a detailed manner.

2. MATERIALS AND METHODS

2.1 Collection and Transesterification of WCO

WCO is less expensive and available in abundant quantities, as it is a by-product. Discarding WCO may lead to significant environmental hazards, soil degradation, and water contamination. Adding value to WCO may lead to its utilization as a feedstock, which will be a boon for the energy sector. In the present investigation, 15 liters of WCO were acquired from the

nearby restaurants in Padur, Chennai, Tamil Nadu, India. The entire content was filtered using a 5-micron sieve to separate it from unwanted remains of the cooking products. Further, a 2-micron filter was used to remove any impurities.

The filtered WCO was subjected to the titration method using phenolphthalein to assess the amount of Free fatty acid (FFA) content. The test revealed the presence of FFA at about 1.8%; therefore, a single-stage transesterification process was adopted using NaOH and methanol. Primarily, 2.1 g of NaOH was thoroughly mixed with 65 ml of methanol to form a sodium methoxide solution. 500 ml of WCO was heated in a conical flask up to 60 °C, and then sodium methoxide solution was added to it with a stirring action initiated at 400 rpm using a magnetic stirrer for 75 minutes. The mixture was then transferred into a separating funnel, and a settling time of 2 hours was allowed. After the cooling and settling period, a ring-shaped structure was distinctly formed, isolating the WCO biodiesel (WCOB) as the upper layer and glycerol as the lower layer (Muthusamy *et al.* 2018). A rotating knob at the bottom removed the glycerol, and the resultant WCOB was washed with double-distilled water and heated up to 120 °C to remove the moisture in the presence of 2% calcium carbonate. By this process, 11.75 liters of WCOB were derived.

2.2 Nanofluid Preparation

Straight diesel fuel (D100) was used in the CI engine as a reference fuel to evaluate the factory-set emission, performance, and combustion characteristics of the test engine. Waste cooking oil biodiesel was blended with straight diesel in the ratios of 10%, 20%, and 30% in volumetric ratio. As per the engine behaviour and literature, D80WCOB20 (80% of diesel and 20% of WCOB) showed optimistic behavior without any engine modification. Further, an increase in the WCOB concentration deteriorated the combustion behavior, especially during the progressive combustion period, leading to fuel injector clogging, erratic running, and escalated exhaust emissions. Therefore, the B20 fuel blend was adopted with doping of Fe_2O_3 nanoparticles at 50 ppm, 100 ppm, and 150 ppm concentrations. The various test fuel images are shown in Fig. 1.

Table 1. Physicochemical properties of the test fuels

Properties	Units	Straight Diesel	WCO	WCOB	D70 WCOB30	D70 WCOB30 + Fe_2O_3 50 ppm	D70 WCOB30 + Fe_2O_3 100 ppm	D70 WCOB30 + Fe_2O_3 150 ppm	ASTM Method
Density	kg/m^3	830	892	871	842	844	849	851	D1298
Kinematic viscosity	cSt @ 40 °C	2.72	7.32	5.92	3.680	3.874	4.025	4.547	D445
Flash point	°C	52	162	110	69	71	73	75	D93
Fire point	°C	55	173	117	74	75	77	78	D93
Calorific value	MJ/kg	42.83	36.23	40.12	42.017	42.517	43.024	44.125	D2015
Cetane index	-	50	46	48	49	51	53	55	-
Ash content	%	<0.01	<0.02	<0.01	<0.01	<0.01	<0.01	<0.01	-
Pour point	°C	-12	-16	-14	-13	-15	-17	-19	D97

Table 2. Properties of Fe_2O_3 NPs

Properties	Units	Fe_2O_3 NP
Density	kg/m^3	5182
Specific heat	J/kgK	103
Thermal Conductivity	W/mK	17.55
Shape	-	Spherical
Appearance	-	Black
Diameter	nm	9

The SEM images of Fe_2O_3 NPs are shown in Fig. 2. The Fe_2O_3 NP 50 ppm fuel blend was prepared by mixing 50 ml of distilled ethanol with 0.01 mg of Fe_2O_3 nanoparticle suspension. Initially, 0.01 mg of Fe_2O_3 nanoparticle was weighed using a digital balance and mixed thoroughly with 100 ml of deionized ethanol in a sterile conical flask. To prevent agglomeration and sedimentation, the mixture was placed in an ultrasonicator bath at a frequency of 60 Hz at 600 rpm for 45 minutes. Further, 1000 ml of waste cooking oil biodiesel was added to the nanoparticle fluid mixture and subjected to mechanical stirring at 750 rpm for 60 minutes. During the stirring process, 2 ml of sorbitan monooleate surfactant solution was thoroughly mixed to ensure the regimentation and clustering prevention due to high energy and surface area (Adhikesavan *et al.* 2022). The surfactant also ensured that the mixture remained stable without sedimentation. The resultant biodiesel-

diesel-nanoparticle mixture was kept aside for a 7-week study to understand its miscibility and sedimentation, as shown in Fig. 3.



Fig. 1: Test fuel images

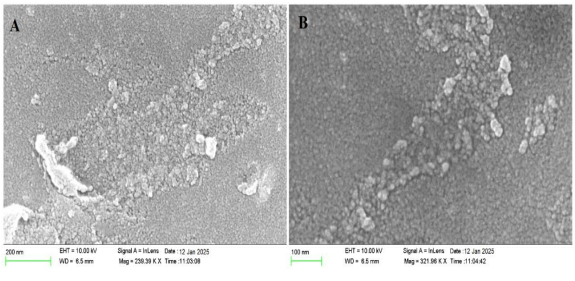


Fig. 2: SEM images of Fe_2O_3 NPs: (A) 200 nm and (B) 100 nm

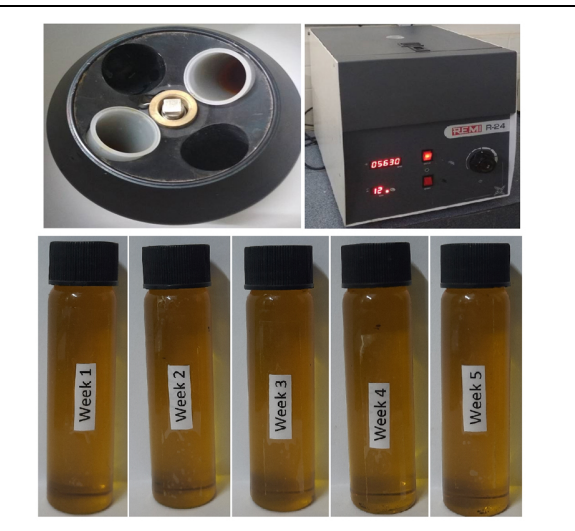


Fig. 3: Nanofluid preparation and Stability analysis

Table 1 details the physicochemical properties of the test fuels employed in the present investigation. WCO, WCOB, D70WCOB, and its nanoparticle-infused fuel with reference to straight diesel are compared. It could be seen that the addition of Fe_2O_3 nanoparticles with WCOB-diesel improved the calorific value and cetane index. Also, an escalation in kinematic viscosity and density can be noted with increasing concentration of Fe_2O_3 nanoparticles. All the other physicochemical properties, including flash-fire point, ash content, and pour point, were determined as per the ASTM procedures and found to be within standards. The properties of Fe_2O_3 were also determined and shown in Table 2. The density and specific heat of Fe_2O_3 nanoparticles were found as 5182 kg/m^3 and 103 J/kg K. Fe_2O_3 nanoparticles are black in color with a spherical shape, measuring 9 nm in diameter, with a thermal conductivity of 17.55 W/mK.

2.3 Engine Specifications

The Kirloskar TV1x single-cylinder test engine was employed in the present investigation. The bore and stroke length of the test engine were 110 mm and 87.5 mm, respectively. The total engine volumetric capacity was 661 cc with a compression ratio of 17.5:1 (Table 3). The load on the engine was accomplished using a water-cooled eddy current dynamometer with a pipe-in-pipe calorimeter to measure the fuel consumption. The engine produces a rated power of 5.2 kW at 1500 rpm. A Kristler pressure transducer with a range of 500 psi, with a low-noise cable, was used to understand the combustion behavior, coupled with a data acquisition system.

Table 3. Test engine specifications

Product	One Cylinder Four-stroke Diesel Engine
Make	Kirloskar, Model TV1x
Bore	110 mm
Stroke	87.5 mm
Compression ratio / Engine capacity	17.5 / 661 cc
Piezo sensor	Range - 5000 psi, with low-noise cable
Calorimeter	Type - Pipe in pipe
Dynamometer	Type eddy current, water-cooled
Rated Power and speed	5.2 kW and 1500 rpm
Cooling arrangement	Water cooling
Load indicator	Digital, Range 0-50 kg, Supply 230 V AC
Load sensor	Load cell, type strain gauge, range 0-50 kg
Air box	M.S., fabricated with an orifice meter and a manometer
Crank angle sensor	Resolution - 1°, Speed - 5500 rpm

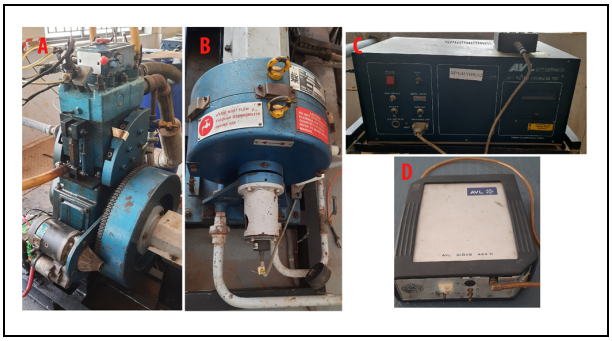


Fig. 4: (A and B) Experimental setup and (C & D) Emission measuring instruments

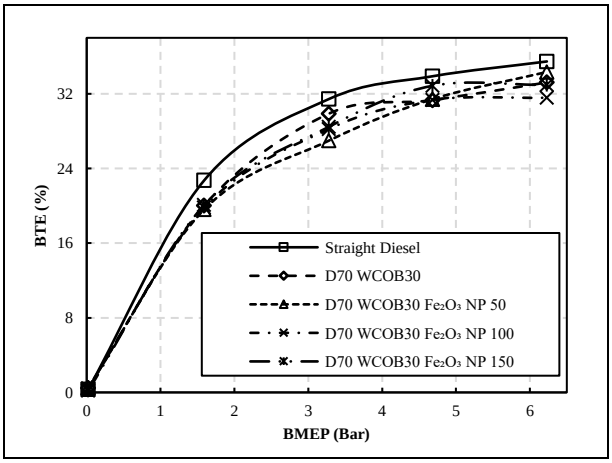


Fig. 5: Variations of BTE

AVL555N Gas analyzer was employed to determine the CO, HC, NO_x, and CO_2, whereas AVL 437C Smoke meter was used to measure the smoke opacity. The time taken for 10 cc fuel consumption was noted along with the engine load and speed at each incremental load, for assessing the BTE and BSFC. Initially, the test engine was operated on straight diesel fuel as a reference. Subsequently, the D70WCOB30 test fuel was used at all load conditions to examine its combustion- and emission-related characteristics. Mechanically agitated D70WCOB30 + Fe_2O_3 NP test fuels were then used one after the other at equal intervals to the engine load. During the test fuel change, the engine was flushed with diesel fuel and operated at part-load conditions for 15 minutes to avoid the residual fuel effect. All test readings were taken thrice, and the average values were plotted. The test engine and the emission measuring instruments are shown in Fig. 4.

3. RESULTS AND DISCUSSION

3.1 Performance Analysis

Fig. 5 depicts the variations of BTE with brake mean effective pressure (BMEP) when fueling the CI engine with straight diesel, D70WCOB30, D70WCOB30 Fe_2O_3 NP50, D70WCOB30 Fe_2O_3 NP100, and D70WCOB30 Fe_2O_3 NP150 test fuels, at all engine loads.

It could be seen that straight diesel had a BTE of 22.72%, 31.45% and 35.47% at low-load, part-load, and full-load conditions. Blending waste cooking oil biodiesel to a 30% volumetric ratio slightly reduced the BTE by 2.78%, 3.01% and 3.34% at low-load, part-load, and full-load conditions, respectively. This may be due to the slight reduction in the calorific value and cetane index of the test fuel with a marginal increase in the kinematic viscosity, preventing the fuel parcels from complete oxidation during the combustion process. Infusing Fe_2O_3 nanoparticles with diesel-waste cooking oil biodiesel showed marginally lower BTE at low-load conditions, but part-load and full-load operations revealed elevated BTE. D70WCOB30 Fe_2O_3 NP 50 showed a BTE of 19.16%, 26.98% and 34.35% at low-load, part-load, and full-load conditions, whereas the same fuel with 100 ppm of Fe_2O_3 NPs showcased 19.81%, 28.23% and 31.58% of BTE at similar engine loading conditions, respectively. This may be due to the superior calorific value of the fuel blends along with improved cetane index. The micro-explosion phenomenon in Fe_2O_3 nanoparticles releasing surplus oxygen atoms, especially at higher engine load, may also be a reason for higher BTE. D70WCOB30 showed higher BTE at part-load conditions, but it deteriorated with escalation in engine load (Yusuf *et al.* 2022; Liu *et al.* 2017).

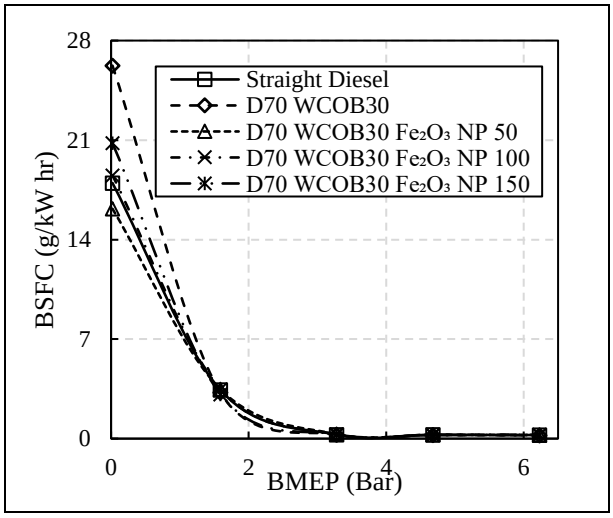


Fig. 6: Variations of BSFC

BSFC *vs.* BMEP plots for the test fuels are shown in Fig. 6. It can be seen that at no-load and low-load conditions, higher BSFC was recorded for all the test fuels, especially with straight diesel, D70WCOB30 Fe_2O_3 NP 100 being the highest. Straight diesel showcased a BSFC of 17.98 g/kWhr, 3.42 g/kWhr, 0.28 g/kWhr, and 0.2545 g/kWhr at no-load, low-load, part-load, and full-load operations, respectively. Diesel-waste cooking oil biodiesel showcased lower BSFC of 26.24 g/kWhr, 3.3287 g/kWhr, 0.2814 g/kWhr and 0.24112

g/kWhr at no-load, low-load, part-load, and full-load conditions, respectively. It can be seen that D70WCOB30 exhibited quite a higher BSFC than straight diesel because of lower energy content. Therefore, a greater quantity of diesel-waste cooking biodiesel would be combusted to produce a similar power output as that of diesel fuel. Doping Fe_2O_3 with diesel–waste cooking biodiesel largely decreased the BSFC initially by 9.23% to 11.04%, but was seen marginally higher at part-load and full-load conditions. Increasing the concentration of Fe_2O_3 NPs in D70WCOB30 further increased the BSFC up to 6.42%. D70WCOB30 Fe_2O_3 NP100 ppm showed a BSFC of 18.52 g/kWhr, 3.12 g/kWhr, 0.321 g/kWhr and 0.2684 g/kWhr at similar loads. D70WCOB30 Fe_2O_3 NP50 has used a relatively low quantity of fuel for producing the same power output due to enhanced combustion, more surface area during the combustion phenomenon, and a relatively higher amount of oxygen atoms, especially at part-load and full-load conditions (Nanthagopal *et al*. 2017; Soudagar *et al.* 2018).

3.2 Emission Analysis

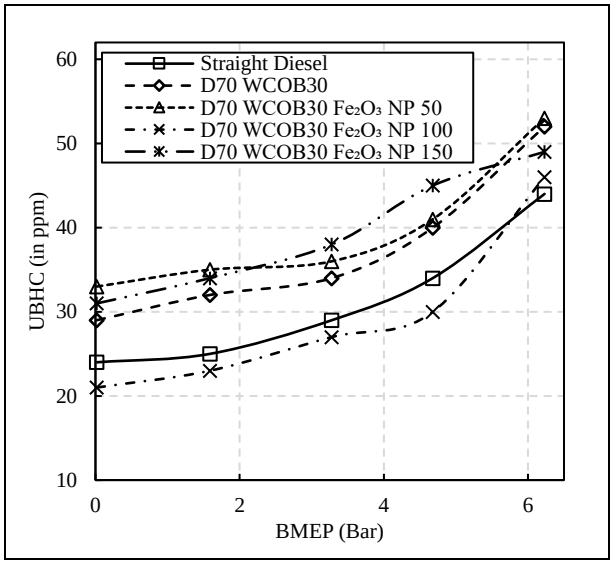


Fig. 7: Variations of UBHC emissions

Fig. 7 depicts the variation in UBHC emissions for the test fuels. Here, the emission data of straight diesel is taken as the reference value. The key reasons for the UBHC formation are the incomplete combustion process, due to improper mixing of air and fuel parcels, locally rich air-fuel mixture, and insufficiency in supplied oxygen molecules. Straight diesel registered an UBHC emission of 25 ppm, 29 ppm, and 44 ppm at low-load, part-load, and full-load operations. Blending WCOB at 30% with straight diesel slightly increased the UBHC formation by up to 4.23% to 6.12% across all loading conditions. This may be due to an increase in fuel density and a reduction in cetane index. Further, the addition of Fe_2O_3 nanoparticles at 50 ppm with D70WCOB30 marginally increased the UBHC emission, especially at part-load and full-load conditions. Rise in kinematic viscosity and cetane index with the addition of Fe_2O_3 may have affected the ignition delay period, which could have resulted in higher formation of UBHC emission. Increasing the concentration of Fe_2O_3 nanoparticles up to 100 ppm significantly reduced the UBHC formation at all loads in comparison to straight diesel and D70WCOB30 fuel blends. This could be due to higher kinematic viscosity, better mixture formation of air and fuel during the diffusive combustion phase. Availability of surplus oxygen due to micro-explosion of nanoparticles at elevated combustion temperature may also be a reason for reduced UBHC formation (Xue, 2013).

Oxides of nitrogen are said to be one of the extremely dangerous emissions arising from the CI engine due to the high-temperature combustion process. NO_x emissions are directly related to the temperature inside the combustion chamber and the availability of mono-atomic and di-atomic oxygen atoms in the combustion space, as they follow the Zeldovich mechanism in the formation of NO, NO_2, NO_3, and N_2O, collectively called NO_x (Subramaniam *et al.* 2013; Samet *et al*. 2023).

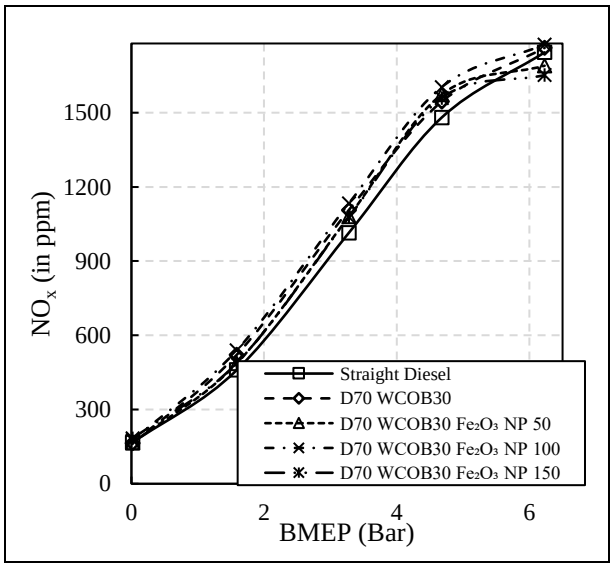


Fig. 8: Variations in NO_x emissions

Fig. 8 shows the variation in NO_x formation across all the test fuel blends in low-load, part-load, and full-load operations. It can be seen that each of the fuel samples follows an upward trend across all the loading conditions. Straight diesel fuel was found to have the lowest NO_x emissions at low-load and part-load, but escalated to the highest level at full load due to the rise in in-cylinder temperature and pressure. D70WCOB30 exhibited a NO_x emission of 522 ppm, 1107 ppm, and 1762 ppm at low-load, part-load, and full-load conditions, respectively. Infusion of Fe_2O_3 NPs at 50 ppm with diesel-waste cooking biodiesel blend slightly

elevated NO_x up to 3.24% at an average across all loading conditions. D70WCOB30 Fe_2O_3 NP100 showcased 540 ppm, 1134 ppm, and 1775 ppm of NO_x emissions at low-load, part-load, and full-load conditions, respectively. The presence of highly reactive mono-atomic oxygen and its strong affinity for atmospheric nitrogen at elevated in-cylinder combustion temperatures, particularly during the premixed combustion stage, may have contributed to higher NO_x formation. Further increasing the Fe_2O_3 concentration up to 150 ppm deteriorated the NO_x formation marginally but was found to be above the levels of D70WCOB30, which may be due to improved miscibility of nanoparticles in the fuel mixture and locally rich air-fuel concentration during the combustion phenomenon. An increase in the surface area due to a higher concentration of Fe_2O_3 may also be a reason for lower NO_x, especially at full-load conditions (Rai and Sahoo, 2024).

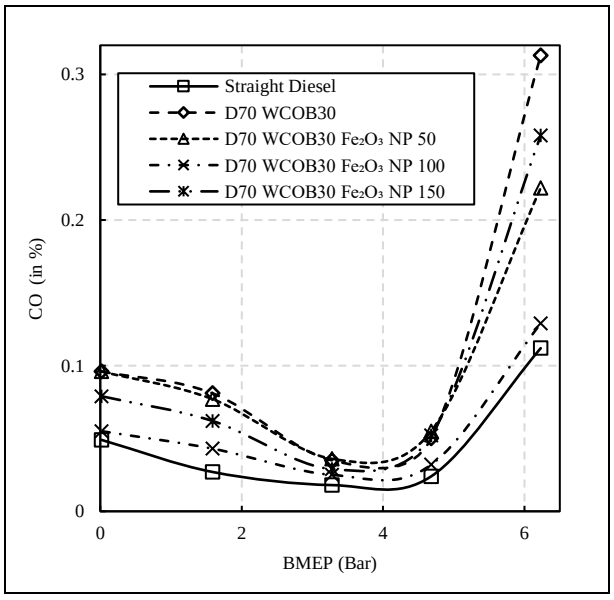


Fig. 9: Variations in CO emissions

The variations in CO formation in a CI engine at all loading conditions when fueled with D70WCOB30 and D70WCOB30 Fe_2O_3 NP50/100/150, along with straight diesel as reference fuel, are plotted in Fig. 9. Initially, at low-load and part-load, the CO emission was in a downtrend and abruptly raised upward, especially during the increase in engine load up to full-load condition. The major reasons for CO formation are the unavailability of an oxygen atom to oxidize the carbon molecules in the fuel parcels and a quicker, progressive combustion process. Straight diesel exhibited a lower amount of CO formation compared to other test fuels, and D70WCOB30 resulted in the highest CO formation. Doping the diesel-biodiesel blend with Fe_2O_3 nanoparticles considerably reduced the CO emission. D70WCOB30 reported CO emission of 0.081%, 0.035% and 0.313%, whereas infusing Fe_2O_3 NP50 fuel emitted 0.077%, 0.036% and 0.222% at low-load, part-load, and full-load operations, respectively. The blend with 100 ppm further reduced the CO formation by 6.08% to 8.94% at full load operation. Higher cetane index and availability of surplus oxygen due to micro-explosion might have led to the complete oxidation of carbon atoms, resulting in reduced CO formation (Sukumar *et al*. 2020; Aydoğan, 2021; Venu *et al.* 2019). Further increasing the concentration of Fe_2O_3 NPs drastically increased the CO formation due to the flame quenching process in the progressive combustion period, as shown in Fig. 9.

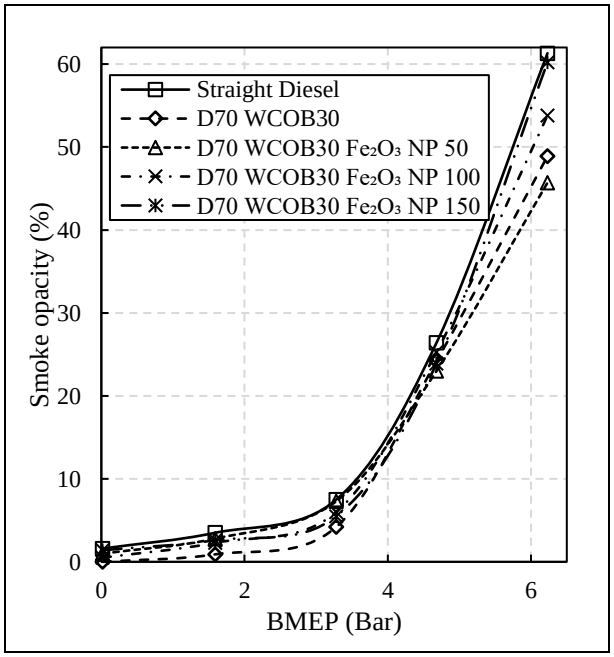


Fig. 10: Variations in smoke opacity

The variation in smoke opacity across multiple test fuel blends at low-load, part-load, and full-load conditions is illustrated in Fig. 10. Incomplete combustion and the unavailability of oxygen atoms during the diffusive combustion phase contribute to smoke formation. In the present study, straight diesel and D70WCOB30 Fe_2O_3 NP150 exhibited higher smoke formation across all loading conditions. Straight diesel exhibited a smoke opacity of 3.51%, 7.53% and 61.32%, whereas D70WCOB30 Fe_2O_3 NP 150 fuel registered 2.6%, 5.56% and 60.54% at low-load, part-load, and full-load, respectively. From these variations, it can be noticed that infusing Fe_2O_3 NPs results in lower smoke formation at low concentration, especially at part-load and full-load conditions. D70WCOB30 Fe_2O_3 NP50 test fuel exhibited the lowest quantity of smoke formation - 2.8%, 7.03% and 45.74% at low-load, part-load, and full-load operations, respectively. Improvements in ignition quality, relatively higher surface activity, and the liberation of surplus oxygen by the nanoparticle resulted in a significant reduction in the smoke formation. The outcome was in line with the findings of Sukumar *et al.* (2020) and Janakiraman *et al*. (2020).

Fig. 11 shows the variations in CO_2 emissions of the test fuels at low-load, part-load, and full-load in a CI engine. All the test fuels showed a similar upward trajectory across all loads in CO_2 formation. Generally, higher CO_2 emissions indicate more complete and efficient combustion. Straight diesel shows a CO_2 emission of 3.45%, 5.07% and 8.85%, whereas D70WCOB30 exhibited 3.44%, 4.99% and 8.68% at low-load, part-load, and full-load conditions, respectively.

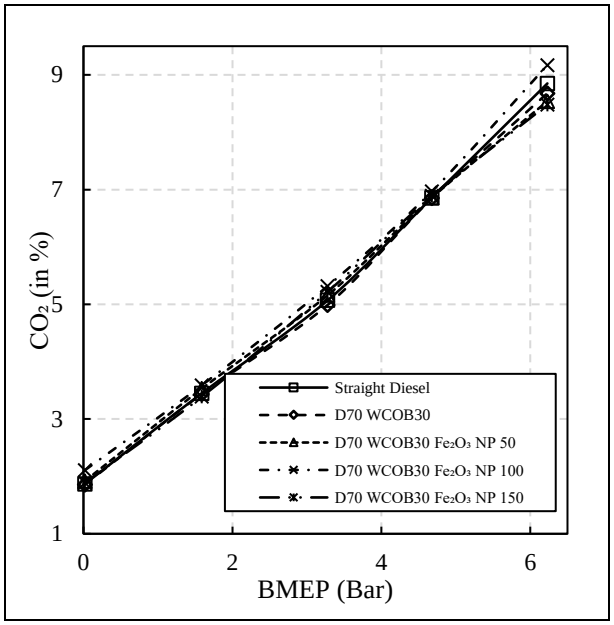


Fig.11: Variations in CO_2 emissions

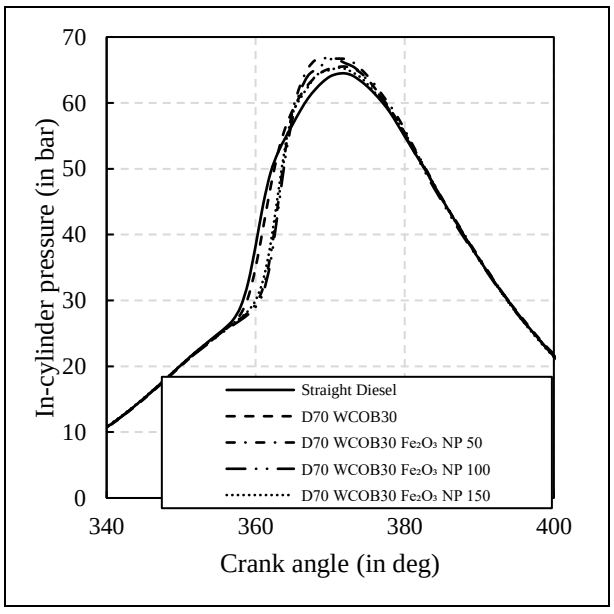


Fig. 12: Variations of in-cylinder pressure

Doping Fe_2O_3 nanoparticle with D70WCOB30 at 50 ppm marginally increased CO_2 formation up to 3.62% to 4.03% at all engine loads. D70WCOB30 Fe_2O_3 NP100 test fuel showcased CO_2 emission of 3.56%, 5.33% and 9.17% at low-load, part-load, and full-load operations. This significant escalation evidenced enhanced oxidation of the carbon atom into CO_2 during the combustion period. Higher energy content of the fuel parcel and improved kinematic viscosity might have led to the increase in CO_2 emissions. It could also be evidenced that an increase in the CO_2 formation effectively balanced the CO formation. On the other hand, a further increase of NPs up to 150 ppm significantly affected the CO_2 formation due to the flame quenching effect and reduced ignition delay period, interfering in the combustion process marginally.

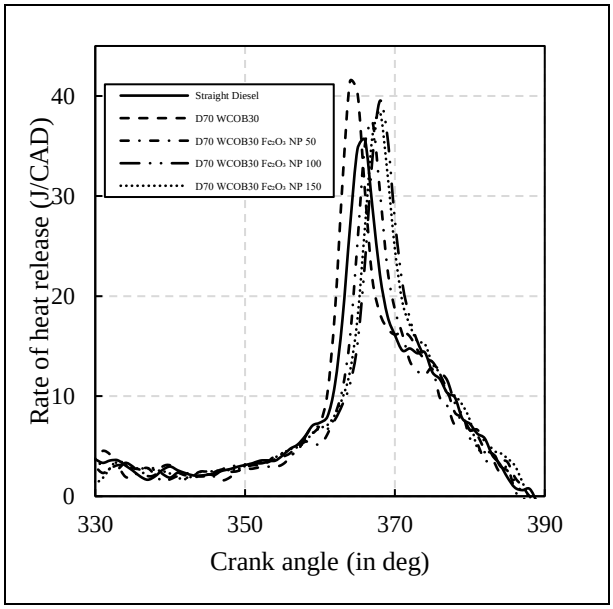


Fig.13: Variations of ROHR

3.3 Combustion Analysis

Fig. 12 shows the variation of in-cylinder pressure of the test fuels at full load conditions. Straight diesel exhibited a higher in-cylinder pressure of 64.19 bar at full-load, whereas D60WCOB30 registered a relatively higher value of 65.509 bar at the same engine load. Availability of an additional oxygen atom, which aided the combustion process, especially during the premixed combustion phase, and the rise in kinematic viscosity, notably leading to enhanced mixing of air and fuel parcels, are the reasons for the increase in in-cylinder pressure. Doping D70WCOB30 with Fe_2O_3 nanoparticle proved to escalate the in-cylinder pressure greatly, as reported by Janakiraman *et al.* (2020) and Sukumar *et al.* (2020) in their studies. 50 ppm and 100 ppm addition of Fe_2O_3 NPs to the D70WCOB30 fuel showed a higher in-cylinder pressure of 66.7908 bar and 66.816 bar, respectively. Rapid combustion due to the liberation of surplus oxygen atoms during the ignition stage initially promoted an enhanced premixed combustion phenomenon. Further addition of Fe_2O_3 nanoparticle up to 150 ppm resulted in a sharp decline in the in-cylinder

pressure up to 65.988 bar at full load condition. This may be due to slower vaporization of the air-fuel mixture, and it can be overcome by advancing the fuel injection timing, which promotes the early combustion process.

Fig. 13 depicts the changes in the rate of heat release (ROHR), expressed in Joules per crank angle degree (J/CAD), when the test fuels were operated at full-load conditions. Straight diesel exhibited an ROHR of 35.619 J/CAD at full load conditions, whereas D70WCOB30 biodiesel blend exhibited an ROHR of 37.43 J/CAD at the same load, which was 3.298% higher. This may be due to higher kinematic viscosity and enhanced energy content in terms of calorific value, along with the inbuilt content of oxygen atoms in the biodiesel fuel. Higher flash point of D70WCOB30 promoted the fuel to burn aggressively, liberating more amount of heat energy. Further, doping the D70WCOB30 with Fe_2O_3 marginally affected the ROHR. It could be observed that Fe_2O_3 at lower concentrations actively participated in the combustion process, especially during the diffusive combustion phase, liberating considerably more heat energy due to the micro-explosion phenomenon. At the same time, an increase in nanoparticle concentration marginally deteriorated the premixed combustion stage, thus resulting in a slower rate of combustion process. A rise in kinematic viscosity and fuel density for Fe_2O_3-doped test fuel may be the reason for the relatively lower ROHR.

4. CONCLUSION

The waste cooking oil biodiesel was derived using a single-stage transesterification process on WCO. Experiments were carried out in a CI engine by using the test fuels, including Fe_2O_3 nanoparticle-doped diesel–WCOB biodiesel blends.

- 15 liters of waste cooking oil were subjected to single-stage transesterification using NaOH and methanol, yielding 11.75 liters of waste cooking biodiesel.

- Fe_2O_3 nanofluid was prepared by ultrasonication process at 60 Hz for 45 minutes in the presence of deionized ethanol and sorbitan monooleate.

- The physicochemical properties, like kinematic viscosity, density, calorific value, and cetane index of WCO, WCOD, and their Fe_2O_3 NP blends were estimated and found to be in line with the ASTM standards.

- The Fe_2O_3 nano-particle was also characterized using SEM analysis, and its physical characteristics like density, specific gravity, and thermal conductivity were found as 5182 kg/m^3, 1023 J/kgK, and 17.85 W/mK, respectively. Further, its stability with D70WCOB30 was also analyzed.

- The BTE of D70WCOB30 Fe_2O_3 NP100 was found to be superior - 19.81%, 28.27% and 31.58% at low-load, part-load, and full-load conditions, respectively. The BSFC of D70WCOB30 Fe_2O_3 NP50 was found to have the lowest value.

- UBHC emission was drastically reduced by up to 4.14% for D70WCOB30 Fe_2O_3 NP100 in comparison with straight diesel at all loads, whereas CO emissions exhibited significant escalation with the addition of Fe_2O_3 nanoparticles, by up to 3.43%.

- NO_x emissions exhibited an upward trend at all loads, especially with Fe_2O_3 doping. Higher NO_x was recorded for D70WCOB30 Fe_2O_3 NP100 at all loading conditions.

- Smoke emission was considerably reduced with the addition of Fe_2O_3 nanoparticles, and its 50-ppm concentration recorded the lowest smoke emission.

- Higher in-cylinder pressure was recorded for D70WCOB30 Fe_2O_3 NP50 at full load operation, followed by 100 ppm of Fe_2O_3 concentration.

- Doping Fe_2O_3 nanoparticles up to 100 ppm with diesel-waste cooking biodiesel fuel blend significantly increased the ROHR up to 39.517 J/CAD at full load condition.

At the outset, it can be concluded that WCOB is a potential alternative source of energy to enhance engine characteristics when doped with Fe_2O_3 up to 100 ppm in an unmodified CI engine.

FUNDING

This research received no specific grant from any funding agency in the public, commercial, or not-for-profit sectors.

CONFLICTS OF INTEREST

The authors declare that there is no conflict of interest.

COPYRIGHT

This article is an open-access article distributed under the terms and conditions of the Creative Commons

Attribution (CC BY) license (http://creativecommons.org/licenses/by/4.0/).



REFERENCES

Adhikesavan, C., Ganesh, D. and Augustin, V. C., Effect of quality of waste cooking oil on the properties of biodiesel, engine performance and emissions, *Cleaner Chem. Eng.*, 4, 100070(2022). https://doi.org/10.1016/j.clce.2022.100070

Akram, S., Mumtaz, M. W., Danish, M., Mukhtar, H., Irfan, A., Raza, S. A., Zhen, W. and Arshad, M., Impact of cerium oxide and cerium composite oxide as nano additives on the gaseous exhaust emission profile of waste cooking oil-based biodiesel at full engine load conditions, *Renew. Energy*, 143, 898-905(2019). https://doi.org/10.1016/j.renene.2019.05.025

Alehegn, Y. L., Zeleke, D. S., Hailegorgis, S. M. and Alehegn, Y. L., Effect of Al_2O_3 nano-particle on the performance and emission characteristics of millettia ferruginea (Berbera) biodiesel blend fuel on single cylinder compression ignition engine, *Next Energy*, 8, 100344(2025). https://doi.org/10.1016/j.nxener.2025.100344

Aydoğan, B., Combustion, performance and emissions of ethanol n-heptane blends in HCCI engine, *Eng. Persp.*, 1(1), 6-10(2021). https://doi.org/10.29228/sciperspective.47890

Gad, M. S., Aziz, M. M. A. and Kayed, H., Impact of different nano additives on performance, combustion, emissions and exergetic analysis of a diesel engine using waste cooking oil biodiesel, *Propul. Power Res.*, 11(2), 209-223(2022). https://doi.org/10.1016/j.jppr.2022.04.004

Hoseini, S. S., Najafi, G., Ghobadian, B., Ebadi, M. T., Mamat, R. and Yusaf, T. J. R. E., Performance and emission characteristics of a CI engine using graphene oxide (GO) nano-particles additives in biodiesel-diesel blends, *Renew. Energy*, 145, 458-465(2020). https://doi.org/10.1016/j.renene.2019.06.006

Janakiraman, S., Lakshmanan, T., Chandran, V. and Subramani, L., Comparative behavior of various nano additives in a DIESEL engine powered by novel Garcinia gummi-gutta biodiesel, *J. Cleaner Prod.*, 245, 118940(2020). https://doi.org/10.1016/j.jclepro.2019.118940

Liu, H., Ma, X., Li, B., Chen, L., Wang, Z. and Wang, J., Combustion and emission characteristics of a direct injection diesel engine fueled with biodiesel and PODE/biodiesel fuel blends, *Fuel*, 209, 62-68(2017). https://doi.org/10.1016/j.fuel.2017.07.066

Mubarak, M., Hussain, J., Shijas, K. M., Juvaid, T., Shahil, N. M., Shadin, A. M. and Duraisamy, B., Investigation on the use of ternary blends of rubber seed–Waste cooking oil biodiesel and diesel as fuel in unmodified diesel engine, *Next Res.*, 2(2), 100311(2025). https://doi.org/10.1016/j.nexres.2025.100311

Muthusamy, S., Nallathambi, S. S., Kumar, R. R. and Mohamed, S. T., Effects of nanoparticles blended biodiesel on single cylinder CI engine, *Mater. Today: Proce.*, 5(2), 6831-6838(2018). https://doi.org/10.1016/j.matpr.2017.11.343

Nanthagopal, K., Ashok, B., Tamilarasu, A., Johny, A. and Mohan, A., Influence on the effect of zinc oxide and titanium dioxide nanoparticles as an additive with Calophyllum inophyllum methyl ester in a CI engine, *Energy Convers. Manage.*, 146, 8-19(2017). https://doi.org/10.1016/j.enconman.2017.05.021

Prabu, A., Premkumar, I. I. and Pradeep, A., An investigation on the performance, combustion and emission characteristics of CI engine on the addition of antioxidants, oxygenates and nanoparticles as additives in Jatropha biodiesel, *Int. J. Amb. Energy*, 41(2), 121-128(2020). https://doi.org/10.1080/01430750.2018.1443281

Rai, R. and Sahoo, R. R., Analysis and optimization of operational and pollutant attributes of diesel engine with CNT-infused orange peel biodiesel-diesel blend fuel, *J. Therm. Sci.*, 33(2), 761-778(2024). https://doi.org/10.1007/s11630-024-1926-z

Samet, U. S. L. U., Duraid, F. M. and AL-GBURI, A. S. K., Synthesis of spirulina microalgae biodiesel, and experimental research of its effects on compression ignition engine responses with iron II-III oxide (Fe3O4) nanoparticle supplementation, *Energy Convers. Manage.*, 293, 117457(2023). https://doi.org/10.1016/j.enconman.2023.117457

Sathish, T., Combustion and emission performance analyzes on the blend of waste cooking oil/Azadirachta indica oil biodiesel/carbon nanotubes in diesel engines, *Int. J. Thermoflu.*, 24, 100964(2024). https://doi.org/10.1016/j.ijft.2024.100964

Sonachalam, M., Manieniyan, V., Senthilkumar, R., Ramis, M. K., Warimani, M., Kumar, R. Kedia, A., Khan, T. M. Y. and Almakayeel, N., Experimental investigation of performance, emission, and combustion characteristics of a diesel engine using blends of waste cooking oil-ethanol biodiesel with MWCNT nanoparticles, *Case Stud. Therm. Eng.*, 61, 105094(2024). https://doi.org/10.1016/j.csite.2024.105094

Soudagar, M. E. M., Nik-Ghazali, N. N., Kalam, M. A., Badruddin, I. A., Banapurmath, N. R. and Akram, N., The effect of nano-additives in diesel-biodiesel fuel blends: A comprehensive review on stability, engine performance and emission characteristics, *Energy Convers. Manage.*, 178, 146-177(2018). https://doi.org/10.1016/j.enconman.2018.10.019

Subramaniam, D., Murugesan, A. and Avinash, A., A comparative estimation of CI engine fuelled with methyl esters of punnai, neem and waste cooking oil, *Int. J. Energy Environ*., 4(5), 859-870(2013).

Sukumar, V., Manieniyan, V., Senthilkumar, R. and Sivaprakasam, S., Production of bio-oil from sweet lime empty fruit bunch by pyrolysis, *Renew. Energy*, 146, 309-315(2020). https://doi.org/10.1016/j.renene.2019.06.156

Venu, H., Subramani, L. and Raju, V. D., Emission reduction in a DI diesel engine using exhaust gas recirculation (EGR) of palm biodiesel blended with TiO_2 nano additives, *Renew. Energy*, 140, 245-263(2019). https://doi.org/10.1016/j.renene.2019.03.078

Xue, J., Combustion characteristics, engine performances and emissions of waste edible oil biodiesel in diesel engine, *Renew. Sustain. Energy Rev*., 23, 350-365(2013). https://doi.org/10.1016/j.rser.2013.02.039

Yusuf, A. A., Ampah, J. D., Soudagar, M. E. M., Veza, I., Kingsley, U., Afrane, S., Chao, J., Liu, H., Ashraf, E. and Buyondo, K. A., Effects of hybrid nanoparticle additives in n-butanol/waste plastic oil/diesel blends on combustion, particulate and gaseous emissions from diesel engine evaluated with entropy-weighted PROMETHEE II and TOPSIS: Environmental and health risks of plastic waste, *Energy Convers. Manage*., 264, 115758(2022). https://doi.org/10.1016/j.enconman.2022.115758